Comparison of Very High-Mg Calcite (Protodolomite) and Well-Ordered Dolomite Using High Resolution Powder Diffraction Methods

Jay M. Gregg[1], **Georgina Lukoczki**[2], **David L. Bish**[3], and **Pankaj Sarin**[4]

[1] Boone Pickens School of Geology, Oklahoma State University

[2] Kentucky Geological Survey, University of Kentucky

[3] Department of Chemistry, Indiana University

[4] School of Materials Science and Engineering, Oklahoma State University

Introduction

- High-resolution diffraction data (lab X-ray, synchrotron X-ray, and neutron) were collected for two natural Ca-Mg carbonate samples that represent endmembers in terms of stoichiometry and cation ordering.
- These samples include the Bonneterre Dolomite (Cambrian, Missouri, USA) used here as a dolomite standard and “protodolomite” (Graf and Goldsmith 1956) or very high-Mg calcite (VHMC) (Holocene, Andros Island, Bahamas).
- Both minerals replaced sediments (microbial laminates) deposited in similar peritidal settings.
- The results presented here offer clues to the reaction paths that lead from “protodolomite” or VHMC to ordered dolomite in nature.

Samples used in this study

The “backreef” microbial laminate facies of the Bonneterre Dolomite (Cambrian, Missouri), from a roadcut near Marble Creek (**right**), was studied by Gregg & Shelton (1990).

Holocene carbonate tidal-flat sediments **(below)** on North Andros Island were studied by Shinn *et al*. (1965; 1969). One of their chief observations was the presence of micrometer-scale, calcium rich, disordered “protodolomite”.

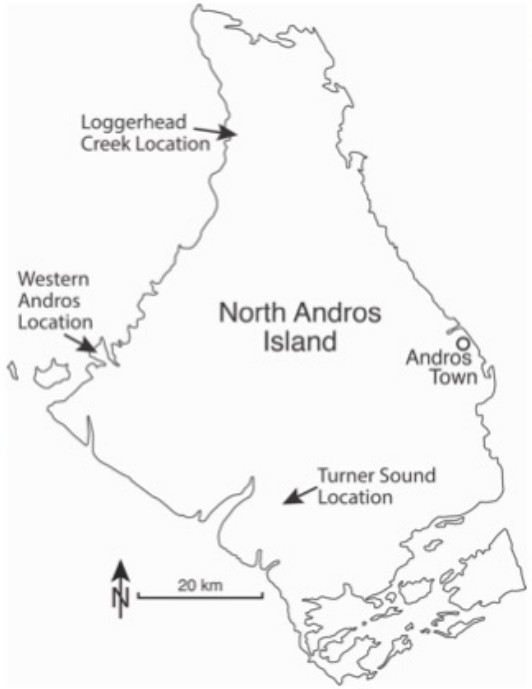

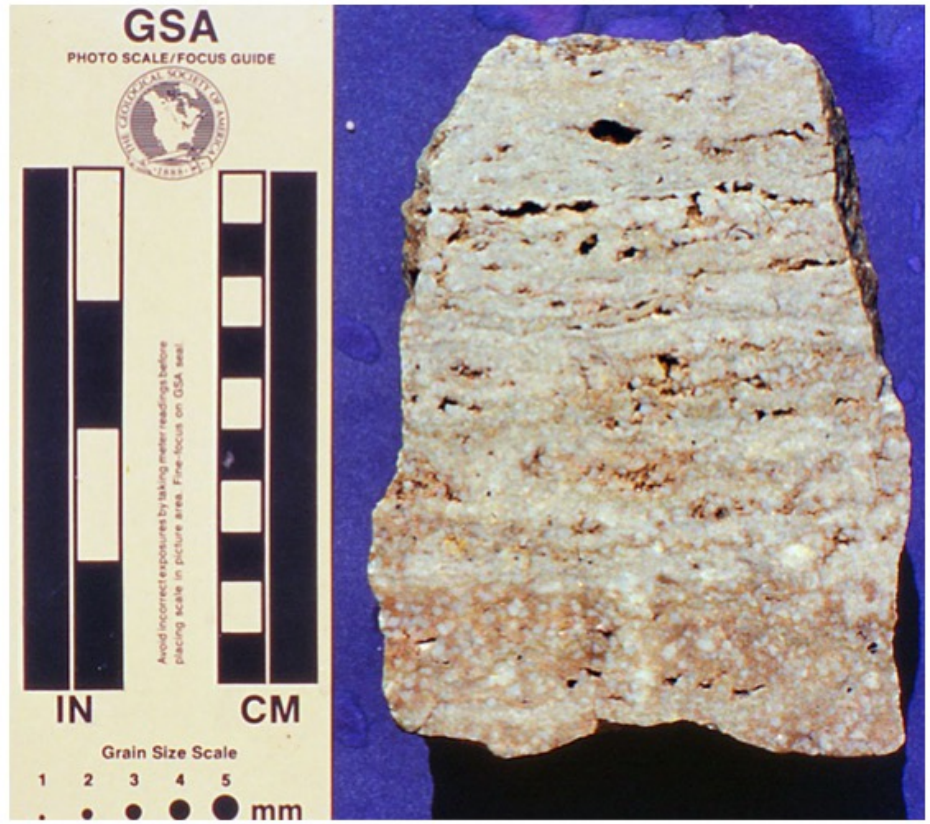

Shinn et al. (1965) studied samples from three locations shown on the map **(left)**. “Protodolomite” replaced up to 80% of pelleted carbonate mud and associated microbial laminates. The ages of the samples range from 0 to ~2300 years (^{14}C analysis).

Samples used in this study

Below: Thin-section photomicrograph of the Cambrian sample displaying course nonplanar texture. Previous studies by Gregg and Shelton (1990) indicate that the dolomite has undergone at least two (early and late diagenetic) recrystallization episodes. Electron probe and ICP-MS bulk analyses indicate near stoichiometry and <0.1 mole percent $FeCO_3$ or $MnCO_3$ composition.

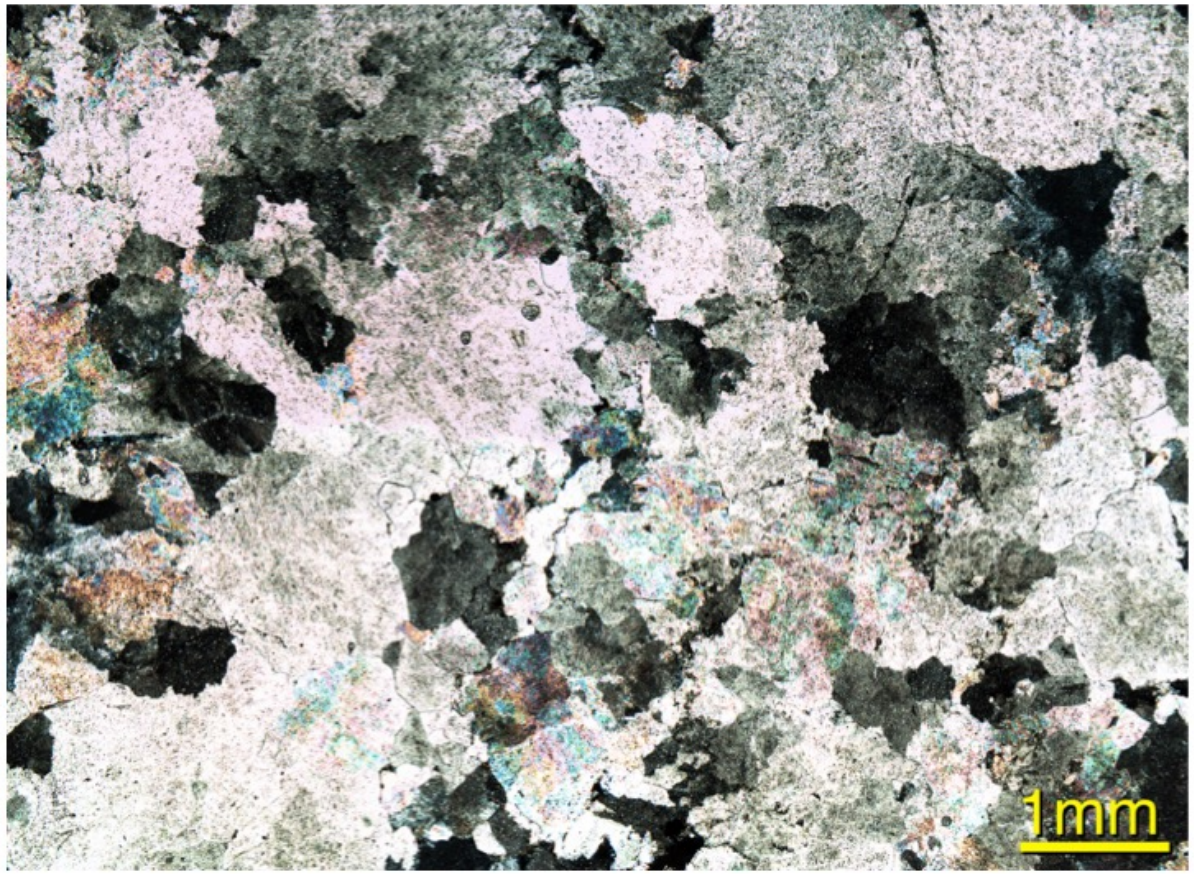

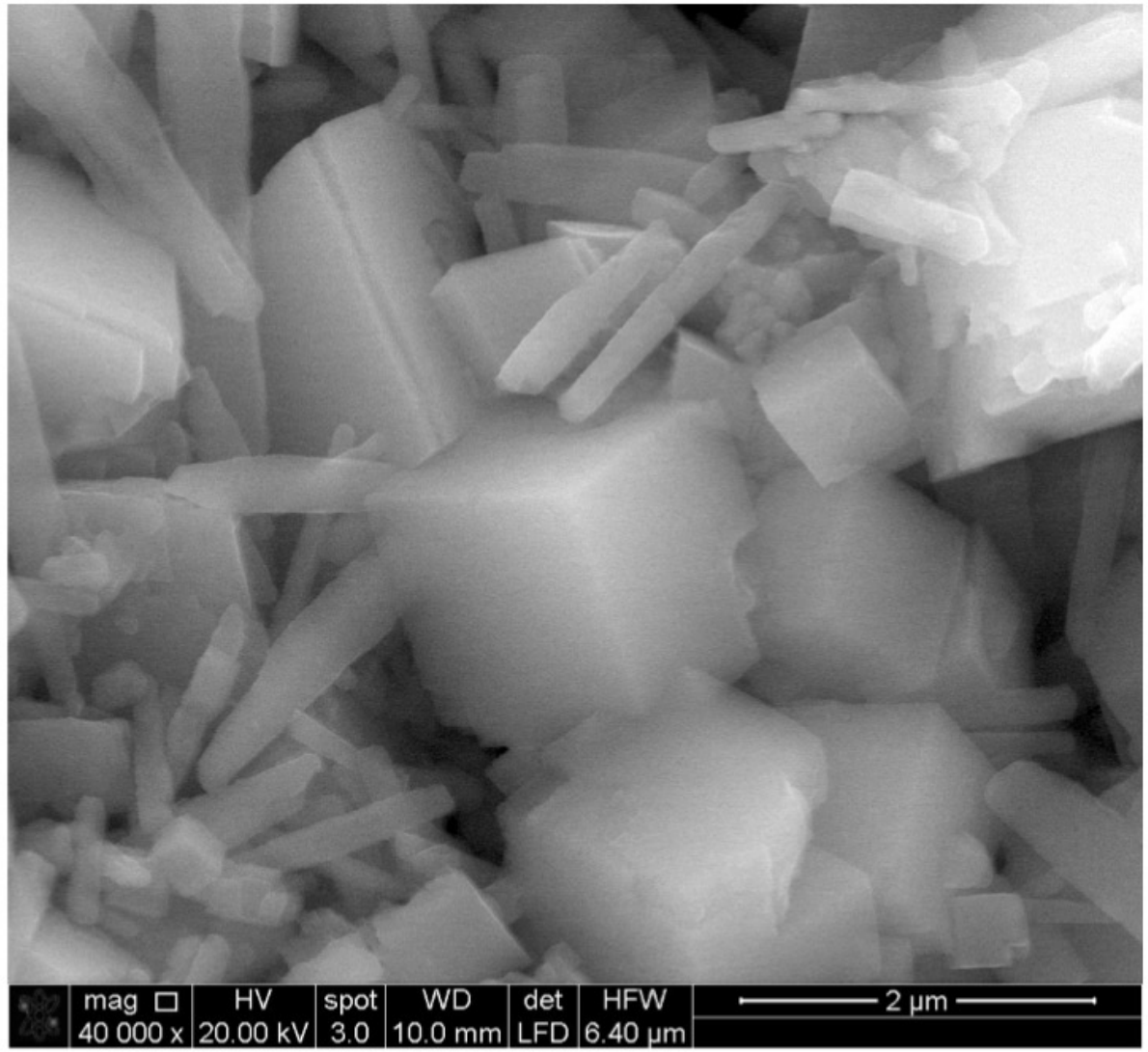

Above: FESEM photomicrograph of the Holocene sample showing "protodolomite" replacing aragonite. Quantitative EDS indicates excess Ca^{2+} with Fe^{2+} and Mn^{2+} below the detection limit. This is confirmed by ICP-MS bulk analyses.

Data used in this study

- **Lab X-ray diffraction (XRD)**
  Bruker D8 Advance X-Ray Diffractometer
  Oklahoma State University Microscopy Facility, Stillwater, OK
- **Synchrotron X-ray diffraction**
  Advanced Photon Source (APS), Beamline 11-BM
  Argonne National Laboratory, Lemont, IL
- **Neutron powder diffraction**
  Center for Neutron Research
  National Institute of Standards and Technology (NCNR), Gaithersburg, MD

Diffraction patterns for calcite & dolomite

Diffraction produces a pattern comprised of reflections (peaks) that represent planes of atoms in a crystalline solid. The 2θ angles are related to the interplanar spacings in accordance with Bragg's law. The numbers labeling the peaks are the Miller-Bravais indices {*hkl*} of the planes.

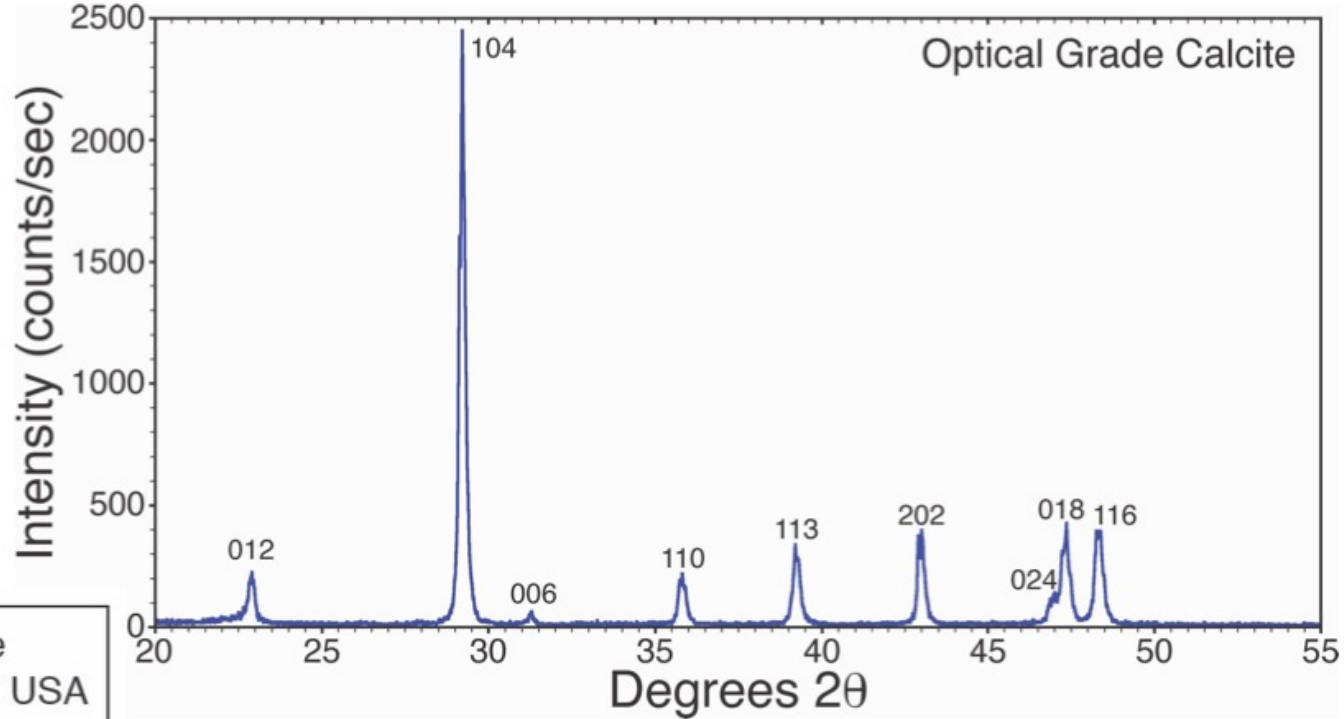

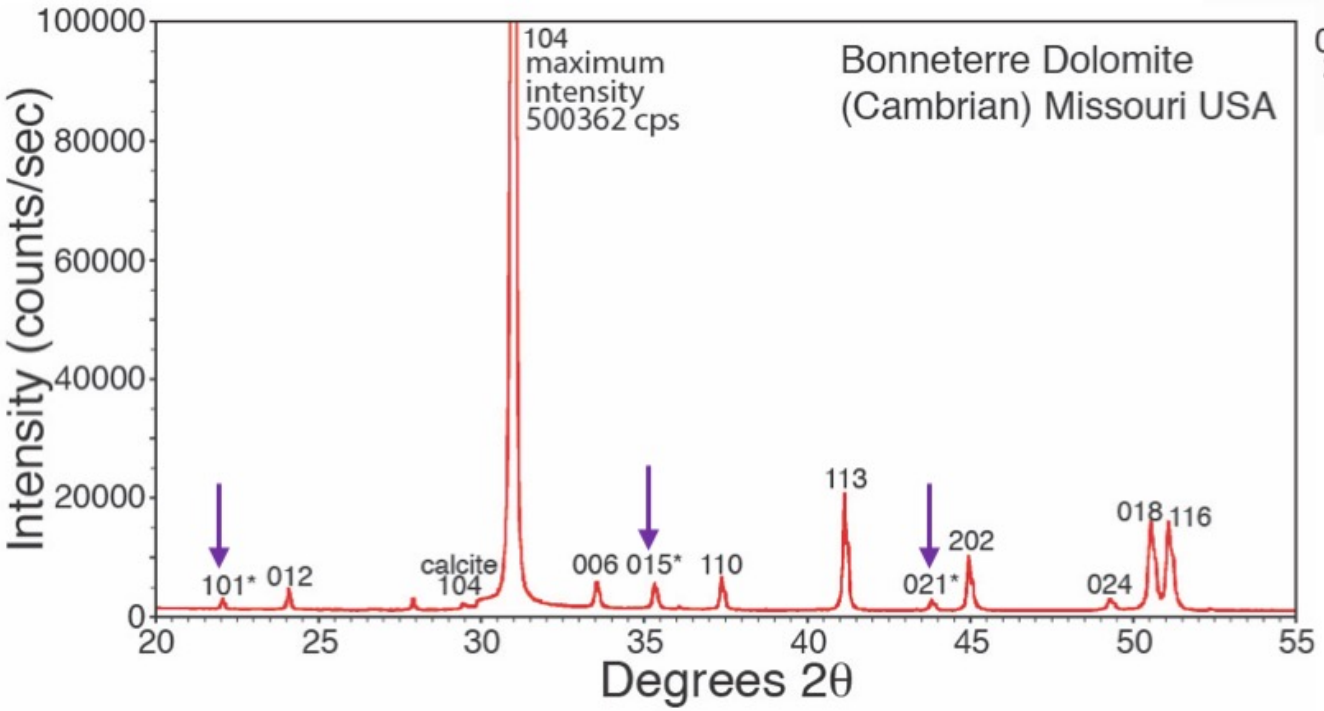

The dolomite and calcite patterns differ due to a set of additional peaks 101, 015, and 021 (purple arrows) that result from the ordering of Mg^{2+} and Ca^{2+} cations into alternating layers normal to the *c* axis. This ordering changes the space group symmetry from $R\bar{3}c$ (calcite) to $R\bar{3}$ (dolomite).

What do diffraction reflections (peaks) represent?

Each reflection or peak corresponds to a repeating plane of atoms that diffract radiation. The 104 and 110 planes exist in both the calcite and dolomite structures. The 015 plane does not exist in calcite. It occurs in dolomite due to the distortion of the carbonate groups caused by the size difference and resulting charge density difference between the Ca^{2+} and Mg^{2+} layers.

104 cleavage rhomb

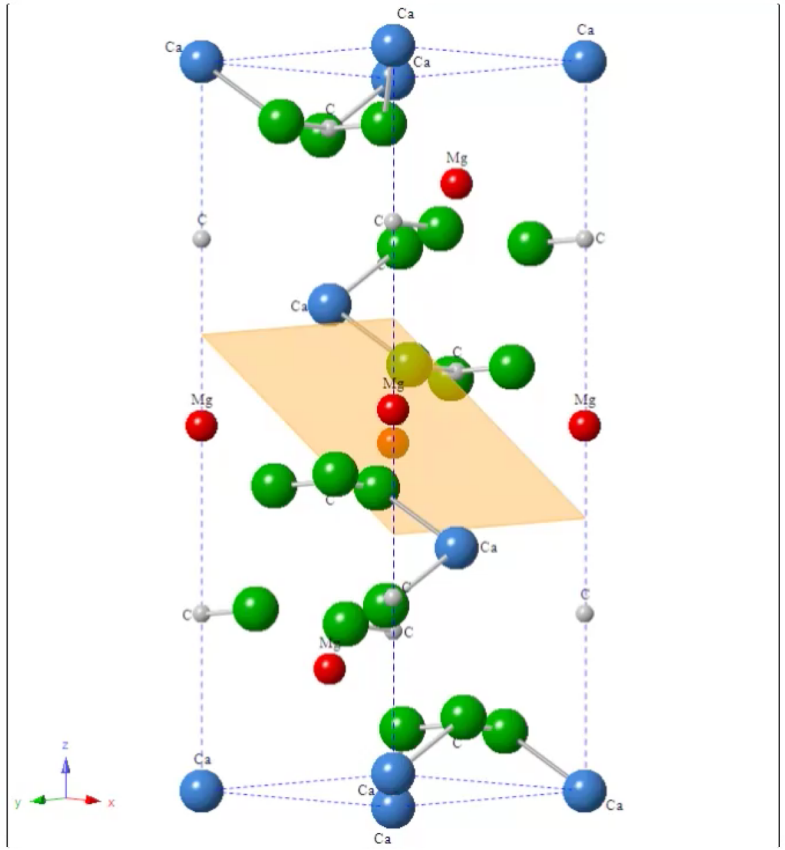

110 prism

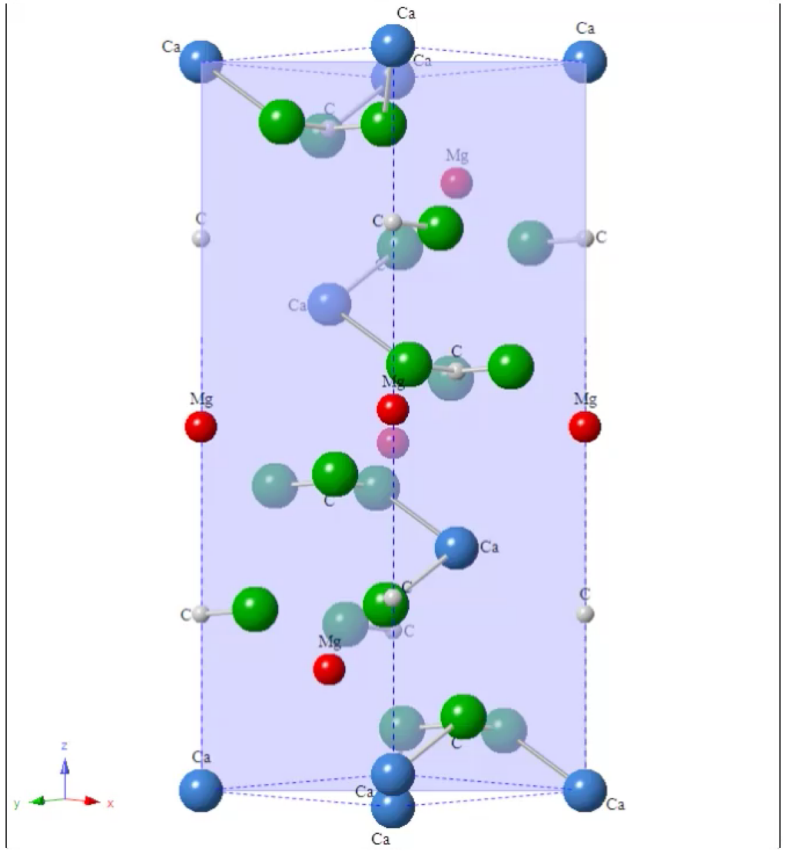

015 “ordering” plane

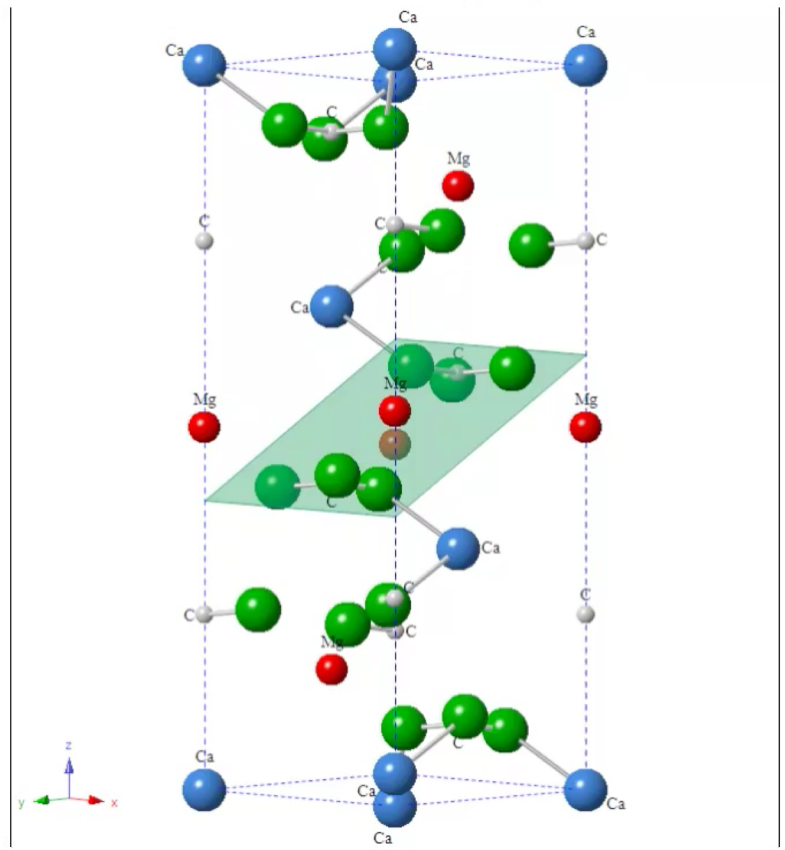

Diffraction analysis

Right: Lab XRD patterns comparing Bonneterre Dolomite with untreated Holocene sediment. “Ordering” reflections are not visible in the Holocene sample.

Below: Long-exposure X-ray powder camera image of Andros Island “protodolomite”. The sample was “cleaned” using a formic acid treatment to remove excess aragonite and calcite prior to X-ray analysis (from Shinn *et al.* 1965). The authors report very faint 221 (015) and 111 (021) “ordering” reflections but they are not visible in the published reproduction shown here.

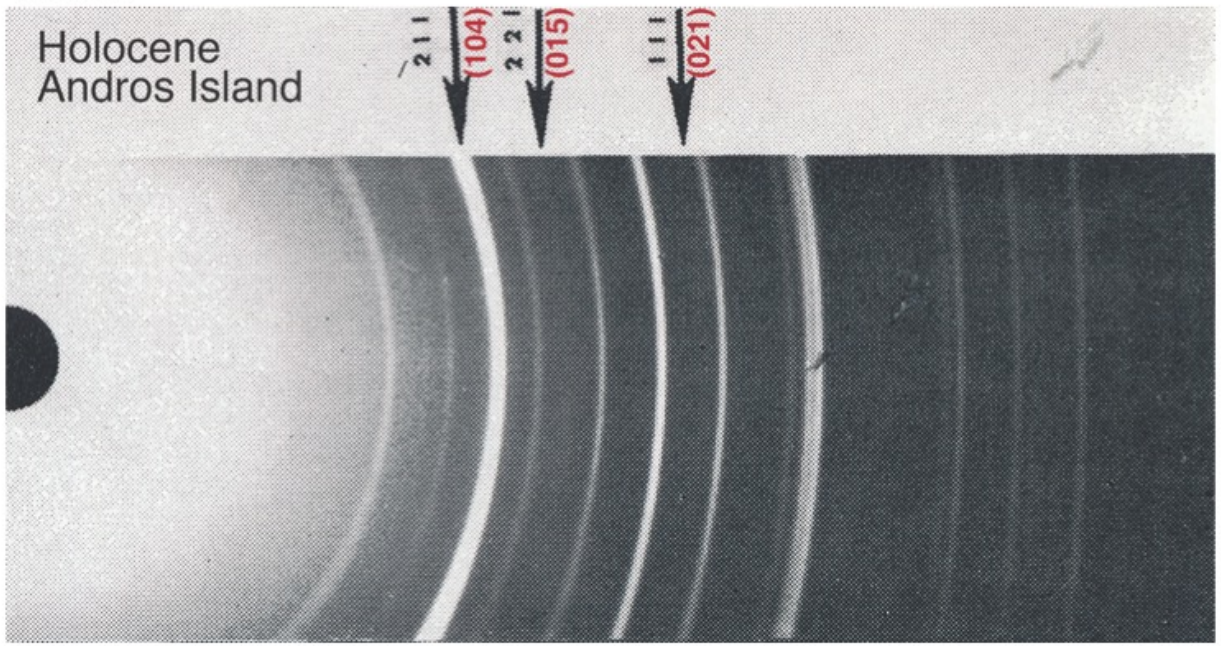

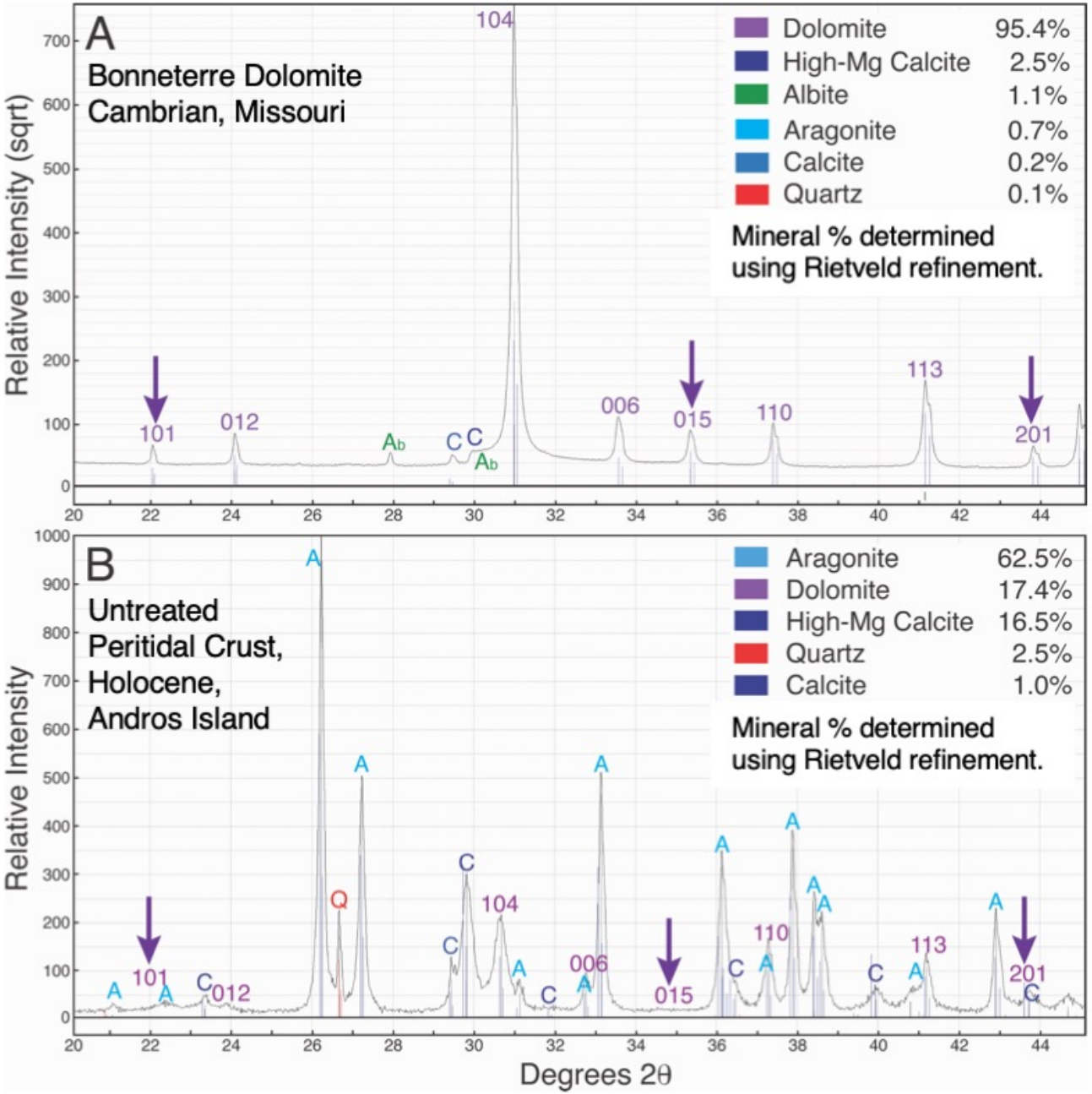

Lab XRD (using Cu*K*α X-rays) and Rietveld refinement of the Bonneterre Dolomite sample treated using disodium EDTA to remove excess $CaCO_3$. Note the relatively close fit between the Rietveld model and the experimental curve. Also note the similarity in the intensities of the 015 and 110 reflections. This is typical of a well-ordered stoichiometric dolomite (Graf and Goldsmith 1956).

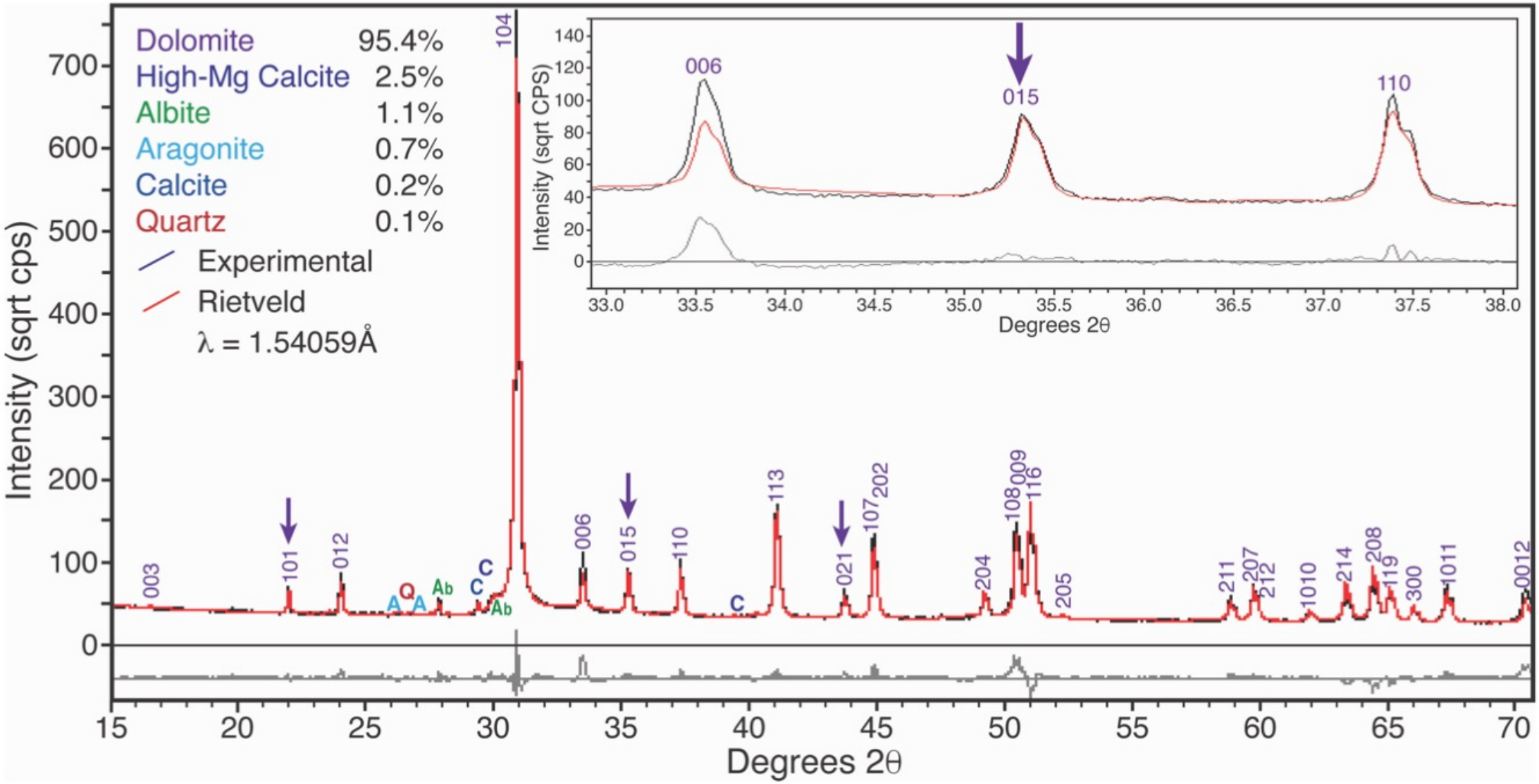

Lab XRD and Rietveld refinement of the Holocene sediment sample treated using disodium EDTA to remove excess $CaCO_3$. Remaining calcite and aragonite peaks are labeled. The very attenuated 110 and 015 "ordering" reflections are represented by broad swells (arrows). The 021 "ordering" reflection, if present, is masked by nearby calcite and aragonite reflections (arrow).

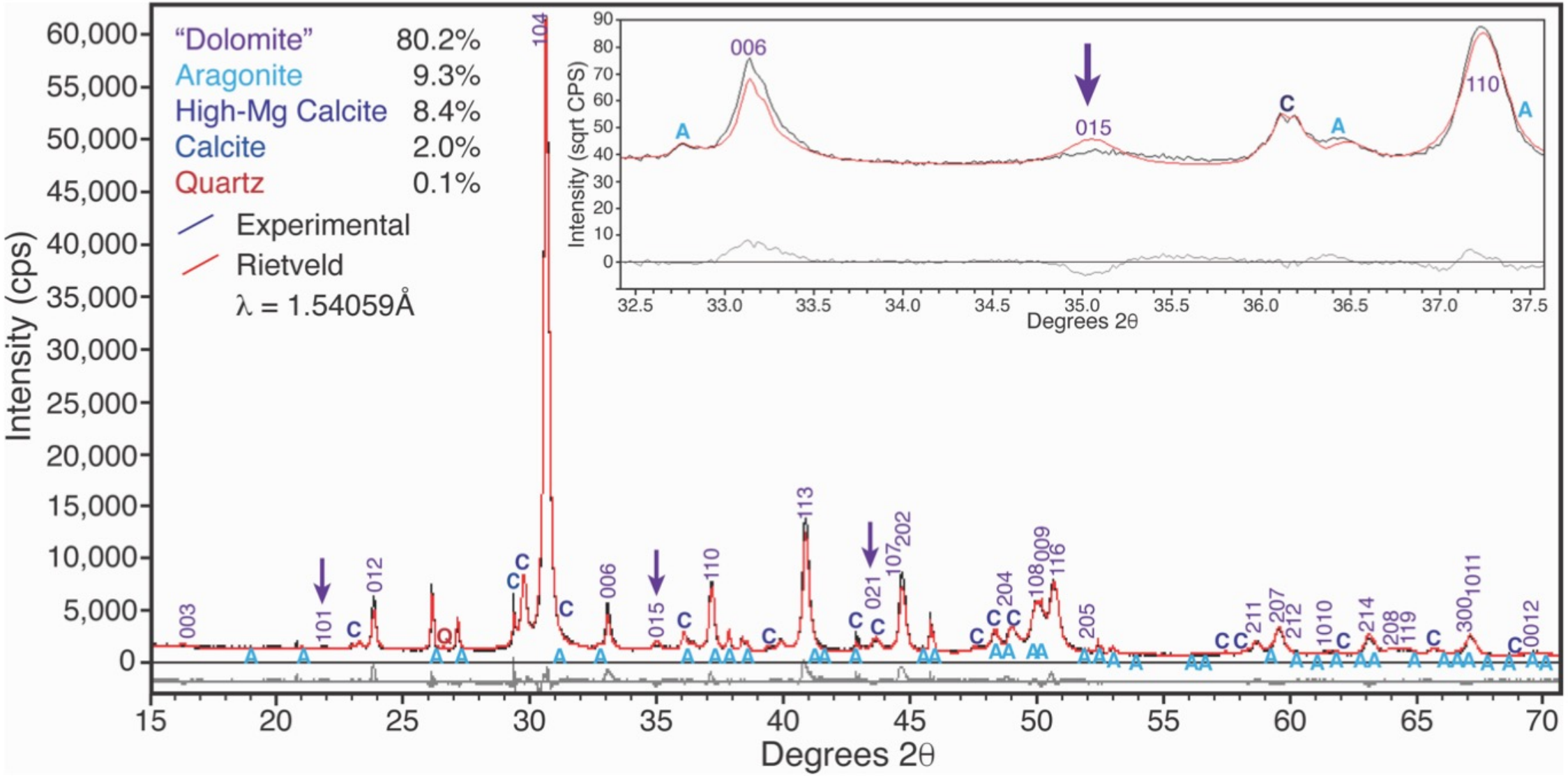

Synchrotron X-ray patterns comparing Cambrian and Holocene samples. Patterns on the left range from 5° to 25° 2θ and on the right from 7.5° to 10.5° 2θ. Arrows show locations of dolomite "ordering" reflections.

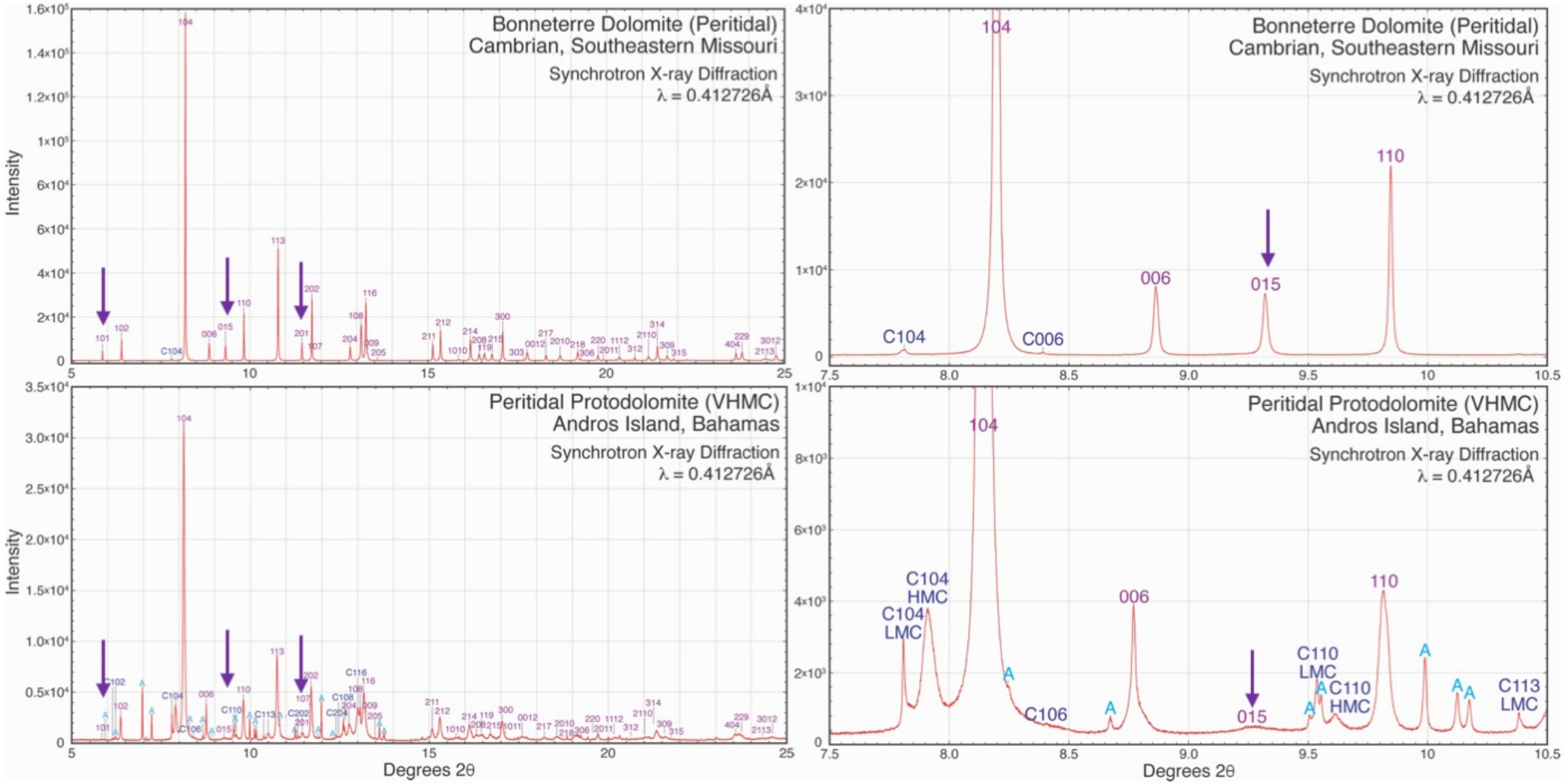

Corresponding **neutron diffraction patterns** comparing Cambrian and Holocene samples. Patterns on the left range from 15° to 75° 2θ and on the right from 29° to 39° 2θ. Arrows show locations of "ordering" reflections. Note lack of "ordering" reflections in the Holocene sample.

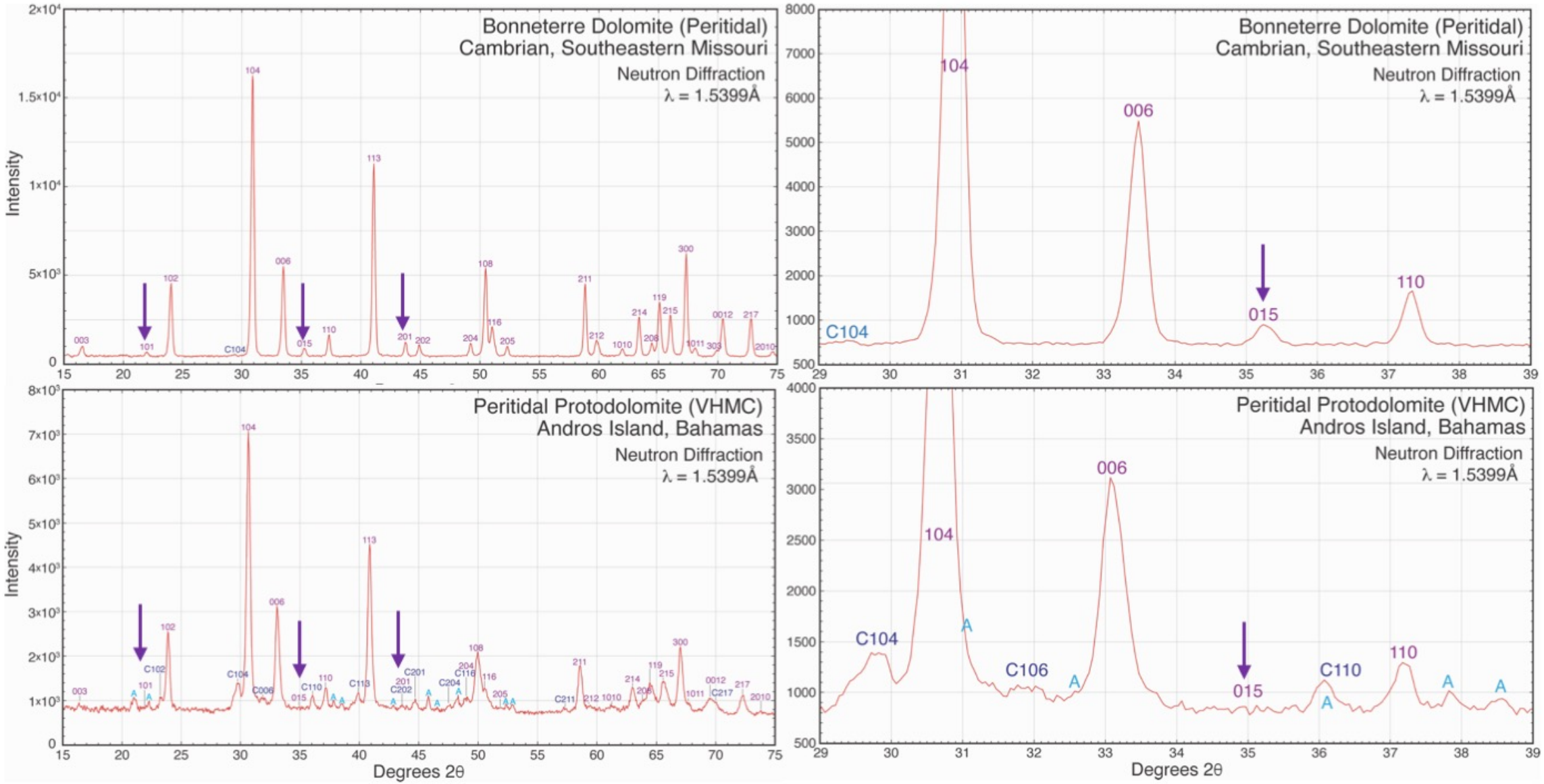

Discussion

Experimental work at >150°C by Sibley *et discipuli* (1987-2014) indicate the reaction pathway to the right. If a similar pathway describes initial nucleation and growth of dolomite in nature, the Holocene specimen represents the nucleation, slow growth, and initial rapid replacement phases as observed in the experimental results shown on the chart.

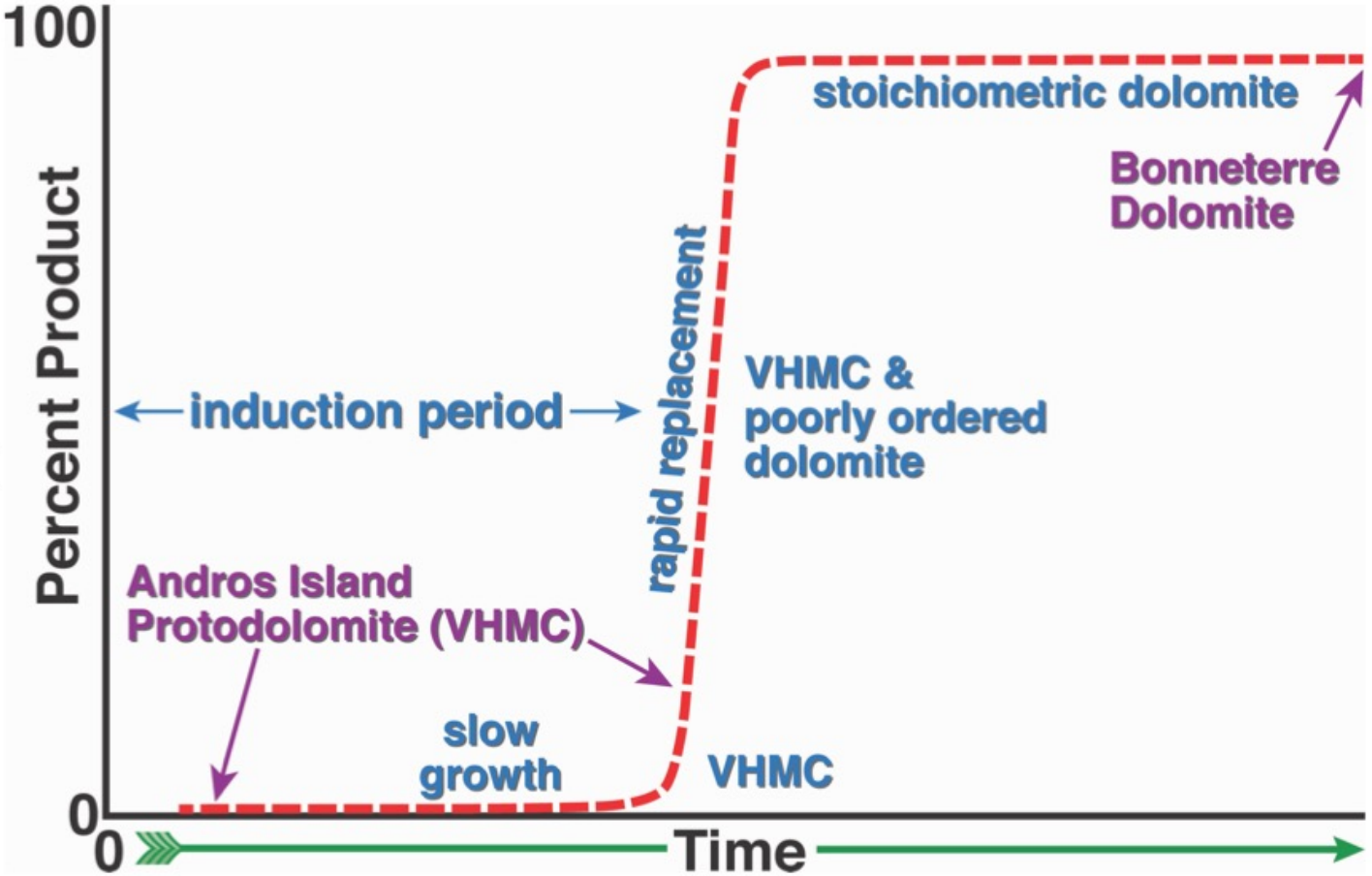

The Cambrian Bonneterre Dolomite represents the end product after repeated recrystallization episodes over time.

The very attenuated ordering reflections observed in the Holocene sample may be caused by scattered domains of cation ordering in an otherwise disordered crystal structure. Possibly similar ordering exists in Ca-Mg carbonate materials synthesized at room temperature in the laboratory but has been unnoticed due to poor quality of X-ray data and interference of accessory minerals preventing identification of incipient ordering reflections.

This poses the question of where exactly do we draw the line between dolomite (with $R\bar{3}$ symmetry) and "protodolomite" or VHMC (with $R\bar{3}c$ symmetry).

Conclusions

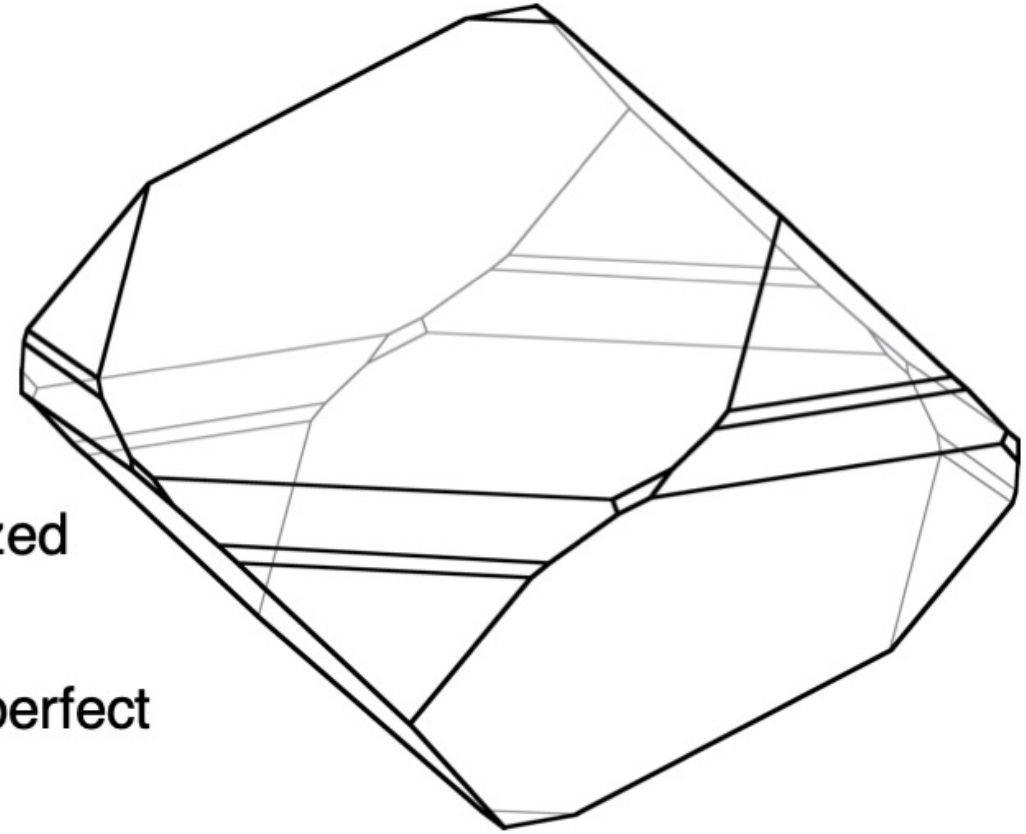

- We present high-resolution diffraction data (lab and synchrotron XRD and neutron) for two Ca-Mg carbonate samples (Holocene and Cambrian) at opposite ends of the dolomite ordering and stoichiometry spectrum.
- Both of these samples have been thoroughly characterized by earlier studies.
- The Cambrian Bonneterre Dolomite sample has nearly perfect stoichiometry and cation ordering.
- The Holocene Andros Island sample displays very attenuated ordering reflections, typically not visible using conventional lab XRD methods. These reflections may be due to scattered domains of cation ordering in an otherwise disordered crystal structure.
- Similar XRD evidence for ordered domains may become visible for Ca-Mg carbonates synthesized at low temperature (with or without microbial catalysis) given better sample preparation and better quality diffraction data.

Questions?

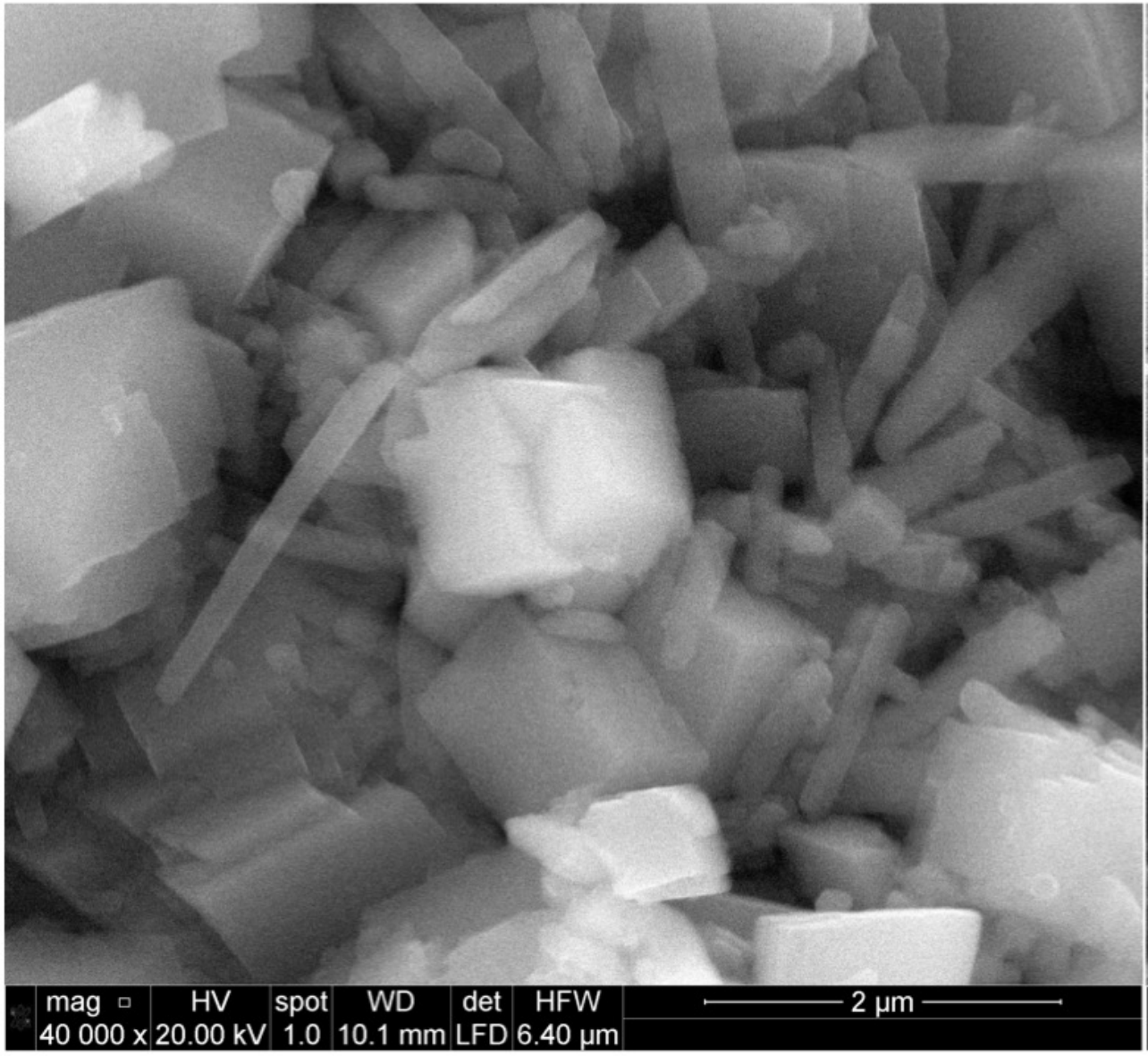
mag
40 000 x
HV
20.00 kV
spot
1.0
WD
10.1 mm
det
LFD
HFW
6.40 µm
2 µm

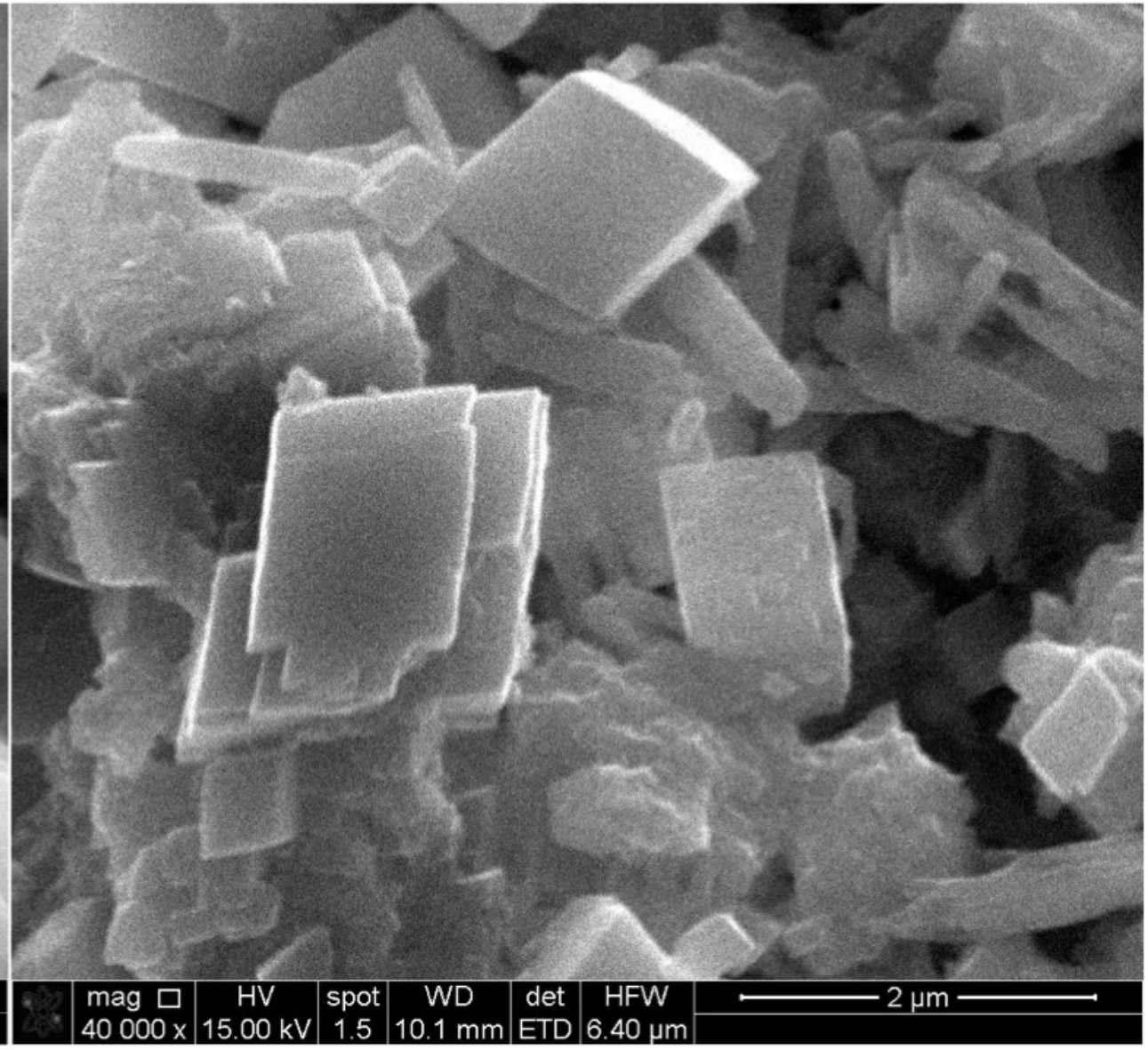
mag
40 000 x
HV
15.00 kV
spot
1.5
WD
10.1 mm
det
ETD
HFW
6.40 µm
2 µm

References

Graf, D. L., and Goldsmith, J. R., 1956, Some hydrothermal syntheses of dolomite and protodolomite: Journal of Geology, v. 64, p. 173-186.

Gregg, J. M., and Shelton, K. L., 1990, Dolomitization and dolomite neomorphism in the back reef facies of the Bonneterre and Davis Formations (Cambrian), southeast Missouri: Journal of Sedimentary Petrology, v. 60, p. 549-562.

Kaczmarek, S. E., and Sibley, D. F., 2011, On the evolution of dolomite stoichiometry and cation order during high-temperature synthesis experiments: An alternative model for the geochemical evolution of natural dolomites: Sedimentary Geology, v. 240, p. 30-40.

Kaczmarek, S. E., and Sibley, D. F., 2014, Direct physical evidence of dolomite recrystallization: Sedimentology, v. 61, p. 1862-1882.

Nordeng, S. H., and Sibley, D. F., 1994, Dolomite stoichiometry and Ostwald's step rule: Geochim et Cosmochim Acta, v. 58, no. 1, p. 191-196.

Nordeng, S. H., and Sibley, D. F., 1996, A crystal growth rate equation for ancient dolomite: Evidence for millimeter-scale flux-limited growth, v. 66, no. 3, p. 477-481.

Shinn, E. A., Ginsburgh, R. N., and Lloyd, R. M., 1965, Recent supratidal dolomite from Andros Island, Bahamas, *in* Pray, L. C., and Murray, R. C., eds., Dolomitization and Limestone Diagenesis: SEPM, Special Publication 13, p. 112-123.

Shinn, E. A., Lloyd, R. M., Ginsburg, R. N., 1969, Anatomy of a modern carbonate tidal-flat, Andros Island, Bahamas: Journal of Sedimentary Petrology, v. 39, p. 1202-1228.

Sibley, D. F., 1990, Unstable to stable transformations during dolomitization: Journal of Geology, v. 98, no. 5, p. 739-748.

Sibley, D. F., Dedoes, R. E., and Bartlett, T. R., 1987, Kinetics of dolomitization: Geology, v. 15, p. 1112-1114.

Sibley, D. F., Nordeng, S. H., and Barkowski, M. L., 1994, Dolomitization kinetics in hydrothermal bombs and natural settings: Journal of Sedimentary Research, v. 64A, no. 3, p. 630-637.